# Spectroscopic Detection of Chemical Intermediates in the Reaction of *para*-Substituted Benzylamines with Bovine Serum Amine Oxidase†

C. Hartmann,‡,§ P. Brzovic,‖ and J. P. Klinman*,‡

*Department of Chemistry, University of California, Berkeley, California 94720, and Department of Biochemistry, University of California, Riverside, California 90024*

*Received August 21, 1992; Revised Manuscript Received December 7, 1992*

ABSTRACT: Anaerobic, rapid-scanning stopped-flow spectroscopy has been used to investigate the UV–visible absorbance changes (300–540 nm) that occur in the spectrum of bovine serum amine oxidase during reduction by benzylamine, *p*-hydroxybenzylamine, and *p*-methoxybenzylamine. The reaction of enzyme with benzylamine generates detectable relaxations at 310, 340, and 480 nm, which are attributed to the production of reduced cofactor (310 and 480 nm) and to an enzyme–substrate Schiff base complex (340 nm). Additional transients have been observed at 440, 425, and 460 nm with *p*-hydroxybenzylamine, *p*-methoxybenzylamine, and *p*-(*N*,*N*-dimethylamino)benzylamine, respectively. These relaxations are ascribed to quinonoid species, formed reversibly from Schiff base complexes between oxidized product and reduced cofactor. With the spectral detection of enzyme–product Schiff base complexes, evidence now exists for each of the postulated chemical intermediates along the reaction path of bovine serum amine oxidase [cf. Hartmann, C., & Klinman, J. P. (1991) *Biochemistry 30*, 4605]. Anaerobic, single-wavelength stopped-flow data, collected in conjunction with rapid-scanning studies for benzylamine and *p*-hydroxybenzylamine, provide approximate rate constants for each of the kinetic processes corresponding to enzyme–substrate Schiff base formation, to enzyme reduction, and to the formation and decay of the quinonoid intermediate.

A novel quinone structure, referred to as 6-hydroxydopa or topa quinone, has been identified as the covalently bound, active site prosthetic group in bovine plasma amine oxidase (BSAO)[1] (Janes et al., 1990). Recent mechanistic probes of BSAO have led to the proposal of a number of reaction intermediates in the deamination of amines to aldehydes catalyzed by protein-bound topa quinone (Janes & Klinman, 1991; Hartmann & Klinman, 1991). As illustrated in Scheme I, evidence exists for the initial formation of a Schiff base complex between substrate and carbonyl of cofactor, species A (Hartmann & Klinman, 1987), followed by proton activation at C-1 of substrate via an active site base (Hartmann & Klinman, 1991). The resulting conjugate acid of the active site base is believed to transfer its proton to the C-4 oxygen in the cofactor ring, driven by large changes in p$K_a$ upon cofactor reduction (Mure and Klinman, unpublished results). This leads to species B which, lacking the electrostatic stabilization present in the initial substrate Schiff base complex, undergoes rapid hydrolysis to the aminoquinol form of reduced topa, species C (Janes & Klinman, 1991). A short lifetime for the product Schiff base complex, species B in Scheme I, is supported by studies of pH-dependent isotope effects in the BSAO catalyzed oxidation of benzylamine (Farnum et al., 1986) and the failure of reductive inactivation experiments to trap any of this species (Hartmann & Klinman, 1987). One of the consequences of the present study is the presentation of spectroscopic evidence in support of species B.

As demonstrated by Palcic and Klinman (1983), the anaerobic conversion of $E_{ox}$ to $E_{red}$ by benzylamine, *m*-tyramine, and dopamine can be monitored at 480 nm, yielding a single-exponential rate process which is a function of substrate concentration. These studies provided an estimate for the intrinsic isotope effect in the proton abstraction reaction of BSAO, as well as showing that measured kinetic constants were in close agreement with calculated constants derived from steady-state isotope effects on $k_{cat}$ and $k_{cat}/K_m$. Recent studies of *p*-hydroxy- and *p*-methoxybenzylamine as substrates have resulted in the unexpected appearance of biphasic traces at 480 nm, indicative of an additional intermediate prior to aminoquinol formation. This type of behavior was originally noted by Olsson et al. (1976) in the reaction of porcine plasma amine oxidase with *p*-methoxybenzylamine, although analysis of their data to obtain rate parameters for the observed processes proved unsuccessful.

As a consequence of the unusual kinetic behavior of benzylamines substituted with electron-releasing substituents, we turned to anaerobic rapid-scanning stopped-flow analyses of BSAO. These studies have allowed absorbance spectra to be monitored between 300 and 540 nm during the course of enzyme reduction by benzylamine, *p*-hydroxybenzylamine, and *p*-methoxybenzylamine. Precedence for the use of rapid-scanning stopped-flow spectroscopy to visualize the entire sequence of events from substrate binding to product formation comes from the work of Drewe and Dunn (1985) and MacGibbon et al. (1987, and references therein). Drewe and Dunn identified the intermediates in the reaction of L-serine with *Escherichia coli* tryptophan synthase, a pyridoxal phosphate-containing enzyme which exhibits some mechanistic similarity to BSAO.

As shown herein, reduction of bovine plasma amine oxidase by benzylamine under anaerobic rapid-scanning stopped-flow conditions leads to a total of three observable transients, attributed to the formation of an enzyme–substrate imine

† This work supported by a grant to J.P.K from the National Institutes of Health (GM 39296).

* To whom correspondence should be addressed.

‡ University of California, Berkeley.

§ Present address: Department of Chemistry, Temple University, Philadelphia, PA 19122.

‖ University of California, Riverside.

[1] Abbreviation: BSAO, bovine serum amine oxidase.

0006-2960/93/0432-2234$04.00/0 

Scheme I: Intermediates in the Reductive Half-Reaction of BSAO[a]

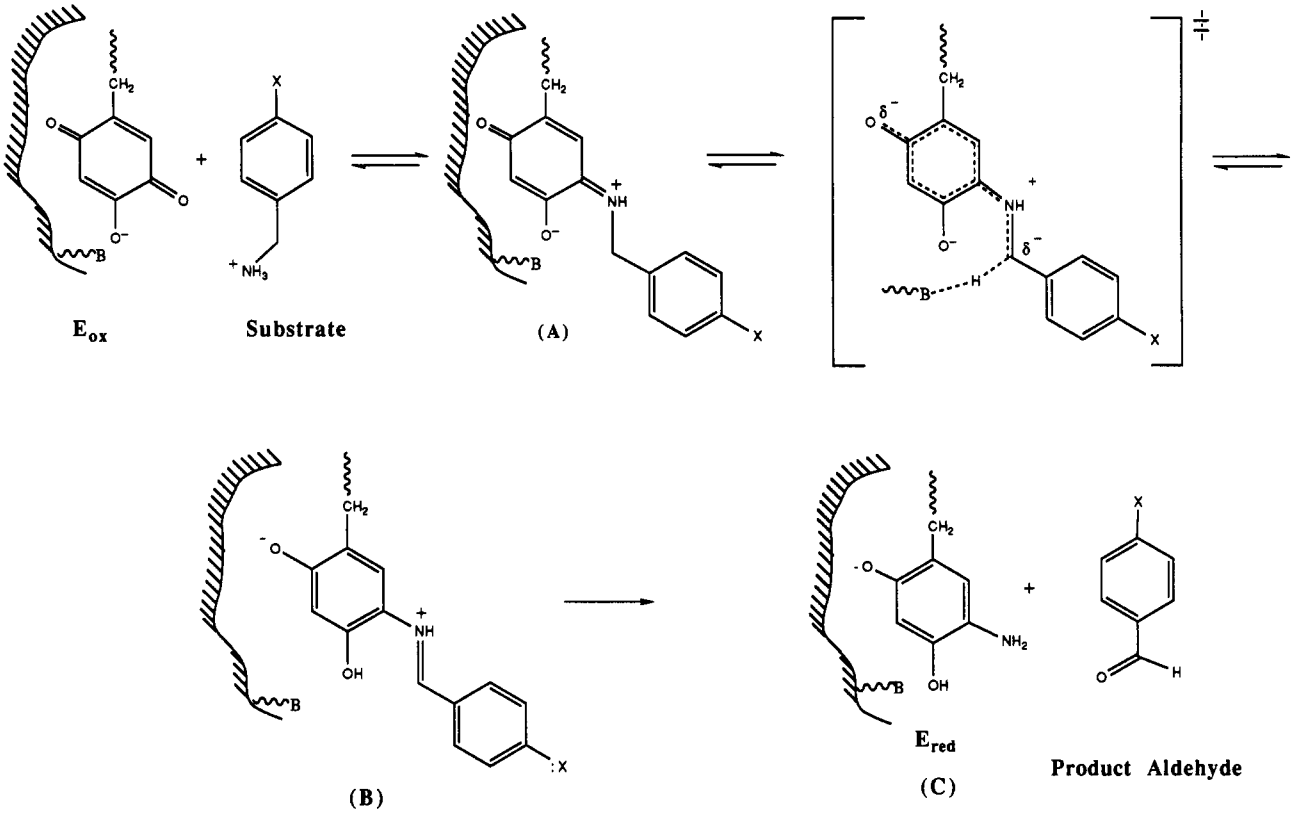


[a] As described in the text, A is the substrate Schiff base complex, B is the product Schiff base complex, and C is the reduced, aminoquinol form of cofactor.

complex (340 nm) and reduction of enzyme-bound cofactor (310 and 480 nm). Reduction of enzyme by *p*-hydroxy-, *p*-methoxy-, or *p*-(*N*,*N*-dimethylamino)benzylamine introduces, in addition, transient accumulation of relaxations centered at 440, 425, and 460 nm, respectively. These new intermediates exhibit spectral properties similar to that of quinonoid intermediates in the tryptophan synthase reaction (Drewe & Dunn, 1985) and in model studies of amines with *para*-substituted benzaldehydes (Csaszar et al., 1978) and of dopa derivatives (Sugumaran & Semensi, 1991). We propose that electron-releasing substituents in the *para*-position of benzylamine facilitate a tautomerization of the enzyme–product imine species. This tautomerization permits the spectral trapping of an otherwise unstable intermediate, species B in Scheme I.

## EXPERIMENTAL PROCEDURES

### *Materials*

All materials were of reagent grade unless otherwise indicated. Bovine plasma amine oxidase was purified by a modification of the procedure of Summers et al. (1979). Enzyme activity and protein concentration were assayed prior to use for anaerobic stopped-flow experiments. Enzyme assays employed 10 mM benzylamine as substrate in 100 mM phosphate buffer, pH 7.2, and were monitored by the increase in absorbance at 250 nm corresponding to benzaldehyde formation. The difference in extinction coefficient of benzylamine and benzaldehyde was taken as 12 800 $M^{-1}$ $cm^{-1}$ (Neumann et al., 1975). Protein concentration was determined spectrophotometrically at 280 nm using an $E^{1\%}_{1cm}$ of 20.8 (Yasunobu et al., 1976). Enzyme activity was normalized to 0.36 units/mg, and rate constants and equilibrium constants were obtained as described under Results. Substrates were synthesized as previously described (Hartmann & Klinman, 1991).

### *Methods*

*Single-Wavelength Stopped-Flow Kinetics.* Anaerobic stopped-flow kinetics were carried out at 25 °C in 100 mM potassium phosphate buffer, pH 7.2, on a modified Aminco-Morrow stopped-flow system and photomultiplier transducer (Kinetic Instruments Inc., Ann Arbor, MI). Rapid data acquisition and subsequent analysis employed an IBM-PC compatible set of hardware and software subsystems. Raw voltage proportional to percent transmission was offset, expanded as necessary, and digitalized via a 12-bit IBM-PC analog-to-digital converter with an on-board crystal-controlled clock to generate precise sampling intervals. Data were stored and analyzed by a program that allows for nonlinear least-squares analysis via a gradient expansion reiterative algorithm to a large number of integral differential equations. The analysis part of the program was supplied by Anarac Assoc. Inc. (1987).

The stopped-flow apparatus was prepared for anaerobiosis by overnight incubation with a solution of 100 mM glucose, 50 units/mL glucose oxidase, and 50 units/mL catalase in 100 mM potassium phosphate buffer, pH 7.2. Anaerobic 100 mM potassium phosphate buffer, pH 7.2, containing the same amounts of glucose, glucose oxidase, and catalase as above, was employed to flush the syringes and chamber prior to use.

For the reductive half-reaction, the anaerobic enzyme was prepared in a tonometer containing enzyme (50–60 $\mu$M) in 100 mM potassium phosphate buffer, pH 7.2, 100 mM glucose, glucose oxidase (50 units/mL), and catalase (50 units/mL).

Substrates were prepared for anaerobiosis by bubbling high-purity argon through 8 mL of phosphate-buffered solutions containing 100 mM glucose in 10-mL disposable syringes for 15 min, followed by the addition of 50 units/mL each of glucose oxidase and catalase.

*Rapid-Scanning Stopped-Flow Spectrophotometry.* Anaerobic rapid-scanning stopped-flow experiments were carried out at 25 °C in 100 mM potassium phosphate buffer, pH 7.2, and were performed on a Durrum D-110 rapid-mixing stopped-flow spectrophotometer modified with a J-Y polychromator and a Princeton Applied Research (PAR) 1412 photodiode array detector. The detector is interfaced with a PAR OMA III multichannel analyzer equipped with a 1463 detector controller card. The hardware configuration for this system has been previously described (Koerber et al., 1983). The stopped-flow apparatus and all solutions used for rapid-scanning stopped-flow were prepared for anaerobiosis as described above for single-wavelength stopped-flow studies.

Data acquisition consisted of collection of a 100% transmission reference spectrum (defined as the light transmitted through the buffer solution used) and the diode array dark current. Utilizing these spectra, rapid-scanning data were initially collected as transmission spectra, converted to absorbance, and stored directly on a floppy disk. The computer software allows 24 spectra to be collected at various intervals. The experiments reported herein utilized 500 pixels on the photodiode array for the repetitive scan time of 8.528 ms/scan with a wavelength resolution of approximately 1 nm. The software of the PAR OMA-III multichannel analyzer allows arithmetic manipulation of the data to yield single-wavelength time courses and difference spectra.

For the spectra reported, the collection of the first scan relative to cessation of flow is noted in the figure legends. Scan delays varied with each experiment and are described below. For Figures 1, 2A, and 5B, the first five scans were collected every 8.528 ms. Subsequent illustrated scans were collected at the following intervals: (7) 204.7 ms; (10) 460.5 ms; (12) 801.6 ms; (15) 1569.2 ms; (20) 3274.8 ms; and (24) 4980.4 ms. In Figures 2B and 5C, the first six scans were collected every 8.528 ms and the seventh through twenty-fourth scans were collected at the following intervals: (7) 59.7 ms; (10) 110.9 ms; (12) 145.0 ms; (15) 221.7 ms; (20) 383.8 ms; and (24) 554.3 ms.

*Anaerobic Single-Turnover UV–Visible Absorbance Spectrophotometry.* To monitor the reductive half-reaction of BSAO by *p*-(*N*,*N*-dimethylamino)benzylamine, a 11.7 μM enzyme solution was prepared for anaerobiosis by incubation in an anaerobic cuvette, under vacuum, with a solution of 50 mM glucose, 50 units/mL of glucose oxidase, and 50 units/mL of catalase in 100 mM potassium phosphate buffer, pH 7.4. The anaerobic cuvette was purged of oxygen by repetitive flushing with argon. The substrate solution was made anaerobic by adding the glucose, glucose oxidase, and catalase cocktail immediately prior to introducing the solution to the side-arm of the anaerobic cuvette. After the substrate was introduced into the side-arm of the cuvette, the entire system was placed under vacuum and repetitively flushed with argon. Substrate was added to the enzyme solution by tilting the apparatus to allow the enzyme solution to enter the side-arm. After this procedure was repeated several times to ensure homogenous mixing, the cuvette was then placed into its holder, and acquisition of spectra was initiated. Data were obtained on a Hewlett-Packard 8450A UV–visible photodiode array spectrophotometer at the following time intervals after mixing: 30, 55, 75, 95, 113, 130, 150, 170, 290, and 590 s.

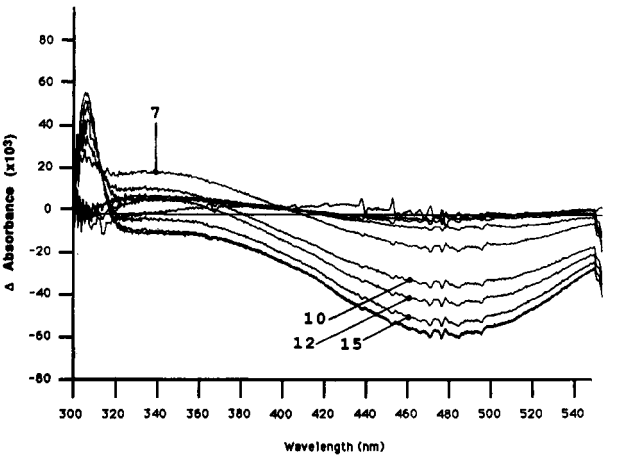


FIGURE 1: Rapid-scanning stopped-flow difference spectra for benzylamine showing the formation and decay of the 340-nm intermediate and the formation of the species at 310 nm, attributed to reduced cofactor. The initiation of scanning occurred 7 ms after flow had stopped. Difference spectra were computed as $(scan)_t - (scan)_0$. Conditions after mixing were 20 mM benzylamine and 45 μM bovine serum amine oxidase in 100 mM potassium phosphate buffer, pH 7.2, 25 °C, in the presence of 100 mM glucose and 50 units/mL of glucose oxidase and catalase. Selective scans have been numbered; timing of the indicated scans is as described under Methods.

Difference spectra were computed as $(scan)_t - (scan)_0$ from the original spectra.

## RESULTS AND DISCUSSION

*Reaction of Bovine Serum Amine Oxidase with Benzylamine.* Rapid-scanning stopped-flow monitoring of the reduction of BSAO by 20 mM benzylamine leads to the difference spectra data in Figure 1, generated by subtraction of the enzyme spectrum from each of the scans. These difference spectra indicate new species arising at 310, 340, and 480 nm during the course of enzyme reduction. In no instance were true isosbestic points observed, either with benzylamine or ring-substituted benzylamines as substrates (see below). Of particular note is the biphasic behavior of the transient at 340 nm, which increases in amplitude until 213 ms (trace 7), after which time it decays. Single-wavelength time courses, reconstructed from the data in Figure 1, confirmed this behavior with absorbance changes consisting of single relaxations at 310 and 480 nm and a biphasic relaxation at 340 nm. Rapid-scanning stopped-flow studies were repeated for [1,1-$^2$H]benzylamine, indicating diminished rates at 310 and 480 nm and little perturbation for the increase in absorbance at 340 nm (data not shown).

Further exploration of the kinetic properties of benzylamine oxidation by BSAO employed single-wavelength stopped-flow analyses at 310, 340, and 480 nm. As summarized in Table I, rate constants measured at 310 and 480 nm are similar with an average value of $2.5 \pm 0.6\ s^{-1}$ for [1,1-$^1$H]benzylamine and $0.17 \pm 0.02\ s^{-1}$ for [1,1-$^2$H]benzylamine. The values of these rate constants and their isotope effects (14.7) are in the range previously measured at 480 nm (Palcic & Klinman, 1983). The similarity of rate constants at 310 and 480 nm (in particular for deuterated substrate) supports the view that both absorbance changes arise from the same process, i.e., the formation of reduced topa. The rate constants for increases in absorption at 340 nm are elevated relative to those for enzyme reduction, with values of 12 and $25\ s^{-1}$ estimated for reduction of protonated and deuterated substrates, respectively. To the extent that kinetic processes are coupled, it is difficult to estimate rate constants for individual transients with great

Table I: Anaerobic Single-Wavelength Stopped-Flow Results for Benzylamine[a]

| substrate | wavelength (nm) | $k_{obs}$ ($s^{-1}$) |
|---|---|---|
| [1,1-$^1H_2$]benzylamine | 480 | 1.90 ± 0.02 |
| | 340[b] (increase) | 12.0 ± 0.7 |
| | (decay) | 1.80 ± 0.11 |
| | 310 | 2.97 ± 0.32 |
| [1,1-$^2H_2$]benzylamine | 480 | 0.17 ● 0.004 |
| | 340[b] (increase) | 25.0 ± 3.5 |
| | (decay) | 0.16 ± 0.01 |
| | 310 | 0.17 ± 0.02 |

[a] Data were collected at 100 mM potassium phosphate buffer, pH 7.2, 25 °C, at a single concentration of 5 mM for both protonated and deuterated amines. Reported $K_m$ values for protonated and deuterated benzylamines are 4.3 and 3.6 mM, respectively (Palcic & Klinman, 1983). [b] Biphasic traces were fitted to the sum of two exponentials: $A_T = A_1(1 - e^{-k_1 t}) + A_2(e^{-k_2 t}) + A_3$.

accuracy. Examination of the data in Table I indicates that the formation fo the 340-nm intermediate yields an inverse isotope effect, which is most likely a result of the difficulty of obtaining pure (uncorrelated) rate constants. Significantly, the absence of a large primary isotope effect on this process contrasts with the behavior at 310 and 480 nm. This property leads to a much cleaner separation of kinetic processes at 310 and 340 nm for reaction of dideuterated than protonated benzylamine. Turning to the data for dideuterated benzylamine in Table I, it can be seen that the decay of the 340-nm band and the appearance of the 310- and 480-nm bands show identical rate constants. This feature implicates the formation of the 340-nm band as a *precursor* to substrate oxidation. Recent model data indicate a $\lambda_{max} = 368$ nm for the formation of an imine complex between a model topa quinone compound and cyclohexylamine (Mure and Klinman, unpublished data). We therefore propose that the 340-nm band in Figure 1 arises from species A, Scheme I. This assignment is consistent with previous studies on BSAO (Hartmann & Klinman, 1987), showing chemical trapping of a Schiff base complex between substrate and the active site cofactor.

*Reaction of Bovine Serum Amine Oxidase with p-Hydroxybenzylamine.* Rapid-scanning stopped-flow data for the reaction of BSAO with 5 mM [1,1-$^2$H]*p*-hydroxybenzylamine showed two additional relaxations when compared with benzylamine (Figure 2). The species absorbing at 330 nm can be easily assigned to *p*-hydroxybenzaldehyde, given the known absorbance properties of this compound (Suva & Abeles, 1978). By contrast, the species absorbing at 440 nm was unanticipated. Figure 2B shows an experiment in which difference spectra were monitored for the first 0.56 s of reaction time (approximately the first 10% of the reaction in Figure 2A). As illustrated, the 440-nm species is quite long lived and does not begin to decay until approximately 400 ms after the start of data acquisition (trace 20). Single-wavelength data, reconstructed from the data in Figure 2, show monophasic exponential increases at 310 and 330 nm (attributed to reduction of cofactor and product formation, respectively) and biphasic behavior at either 440 or 480 nm. As a control for the effect of a ring hydroxy substituent which is unable to conjugate with the carbon undergoing oxidation, rapid-scanning stopped-flow experiments were repeated with tyramine. Using 7 mM substrate, data were virtually identical to those for benzylamine (Figure 1), with no detectable transient at 440 nm.

Rapid-scanning stopped-flow data for [1,1-$^1$H]*p*-hydroxybenzylamine substrate were not obtained, as pure compound was unavailable at the time these experiments were performed. However, in subsequent single-wavelength stopped-flow experiments, a detailed comparison of protonated and deuterated substrates was carried out. Data were collected at 310 and 440 nm over a wide range of substrate concentrations (50 μM–20 mM) under experimental conditions analogous to those used in rapid-scanning stopped-flow measurements. The biphasic kinetic behavior observed at 440 nm is illustrated in Figure 3 for reaction of BSAO with 10 mM [1,1-$^1$H]-benzylamine (A) and [1,1-$^2$H]*p*-hydroxybenzylamine (B). This figure was chosen to show the differences in the accumulation of the intermediate for H vs D substrate at a concentration which was similar to that used for rapid-scanning stopped-flow measurements.

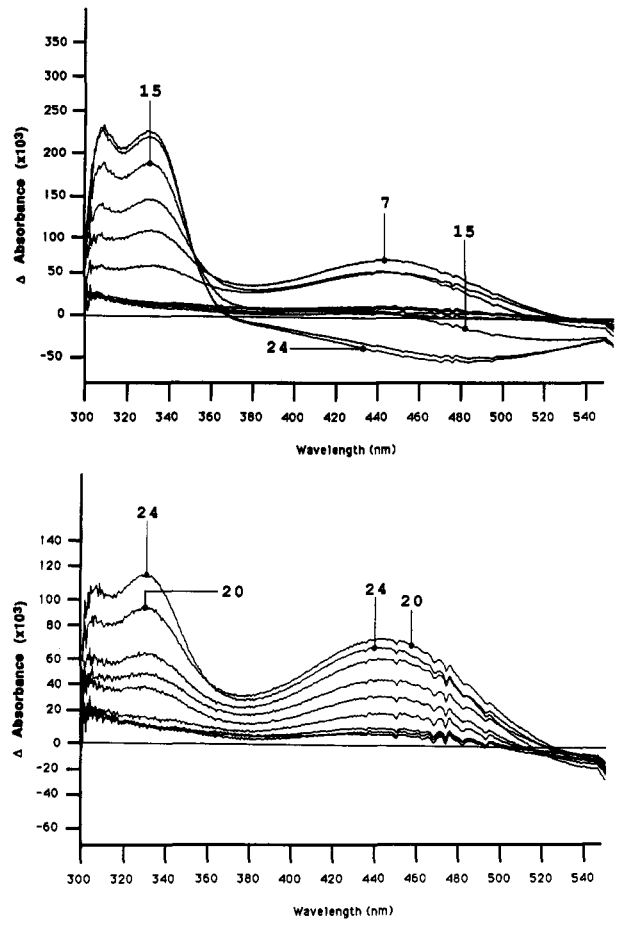


FIGURE 2: Rapid-scanning stopped-flow difference spectra (A, top, and B, bottom) for *p*-hydroxybenzylamine showing the formation and decay of the 440-nm reaction intermediate and the formation of the species at 310 and 330 nm, attributed to reduced cofactor and product aldehyde, respectively. These spectra was measured at 5 mM final concentration of [1,1-$^2H_2$]*p*-hydroxybenzylamine and 36 μM BSAO. The difference between panels A and B is the shorter data acquisition time (0.563 s) in panel B. Selected scans have been numbered; timing of the indicated scans is as described under Methods.

At each substrate concentration, the monophasic increase in absorbance at 310 nm was fitted to eq 1 and the biphasic behavior at 440 nm to eq 2:

$$A_T = A_1(1 - \exp^{-t\lambda_1}) + A_2 \quad (1)$$

$$A_T = A_1(1 - \exp^{-t\lambda_1}) + A_2(\exp^{-t\lambda_2}) + A_3 \quad (2)$$

In eq 2, $A_1$ and $A_2$ are the reaction amplitudes of the two phases; the values of $\lambda_1$ and $\lambda_2$ represent the apparent first-order increase ($k_{inc}$) and decrease ($k_{dec}$) in absorbance at 440 nm, respectively.

Double-reciprocal plots of $1/k_{310}$ vs $1/[S]$ and $1/k_{dec}$ vs $1/[S]$ (440 nm) were found to be linear, whereas the plot of $1/k_{inc}$ vs $1/[S]$ (440 nm) was nonlinear for both protonated

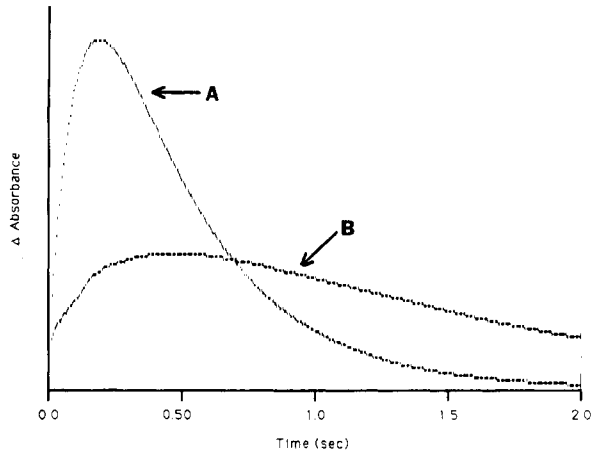


FIGURE 3: Single-wavelength absorbance traces comparing the rate of formation and decay of the spectral intermediates at 440 nm with 10 mM *p*-hydroxybenzylamine (A) and 10 mM [1,1-$^2H_2$]*p*-hydroxybenzylamine (B) and 26 $\mu$M enzyme.

Table II: Parameters Derived from Anaerobic Single-Wavelength Stopped-Flow Studies of [1,1-$^1H_2$]- and [1,1-$^2H_2$]*p*-Hydroxybenzylamine[a]

| substrate | wavelength | $k_{obs}$ ($s^{-1}$) | $K_{app}$ (mM) |
|---|---|---|---|
| [1,1-$^1H_2$]*p*-hydroxybenzylamine | 310 | 38.3 ± 0.6[b] | 3.16 ± 0.24[f] |
| | 440 (increase) | 40.8 ± 1.6[c] | |
| | (decrease) | 6.94 ± 0.13[d] | 0.397 ± 0.003[g] |
| [1,1-$^2H_2$]*p*-hydroxybenzylamine | 310 | 4.41 ± 0.27[b] | 4.27 ± 0.62[f] |
| | | (8.49 ± 0.26)[e] | (0.74 ± 0.085)[e] |
| | 440 (increase) | 1.33 ± 0.01[c] | |
| | (decrease) | 3.38 ± 0.11[d] | 1.80 ± 0.01[g] |
| | | (2.05 ± 0.003)[e] | (0.22 ± 0.01)[e] |

[a] Data were collected in 100 mM potassium phosphate buffer, pH 7.2, 25 °C, using 50 $\mu$M–20 mM substrate. [b] Limiting rate constants, under conditions of substrate saturation. $k_{obs}$ is 2-fold greater than values previously calculated from steady state isotope effects (Hartmann & Klinman, 1991). [c] Values for $k_{obs} = k_2$ estimated by fitting eq 4 to data in Figure 4, with $K_I(H) = 0.32\ mM^{-1}$ and $K_I(D) = 0.23\ mM^{-1}$. [d] Limiting rate constants, under conditions of substrate saturation. [e] Values in parentheses represent deuterium isotope effects. [f] $K_{app} = 1/K_1$. [g] $K_{app} = 1/K_1K_2K_3$ (see text).

and deuterated substrates (data not shown). Kinetic parameters obtained from double-reciprocal plots of data collected at 310 nm are summarized in Table II. Measured isotope effects of enzyme reduction are found to be $^D(k_{310}) = 8.49 \pm 0.26$ and $^D(k_{310}/K) = 11.8 \pm 0.4$ and are in the range of values previously measured for benzylamine [13.5 ± 1.3 (Palcic & Klinman, 1983)] and *p*-(trifluoromethyl)benzylamine and *p*-acetylbenzylamine [11.2 ± 0.8 and 11.4 ± 0.5 (Hartmann & Klinman, 1991)].

The kinetic complexity of the transients at 440 nm precluded a straightforward extraction of limiting kinetic parameters from double-reciprocal plots as a function of substrate concentration. We therefore chose to analyze the data according to the minimal mechanism

$$E_{ox} + S \underset{k_{-1}}{\overset{k_1}{\rightleftharpoons}} E_{ox}S \underset{k_{-2}}{\overset{k_2}{\rightleftharpoons}} E_{red}P \underset{k_{-3}}{\overset{k_3}{\rightleftharpoons}} E_{red}I \qquad (3)$$

$$E_{red}P \xrightarrow{k_4} E_{red}\text{–}NH_2 + S$$

where $k_1$ and $k_{-1}$ represent rate constants for substrate binding and $k_2$ and $k_{-2}$ are rate constants for formation of the product Schiff base complex. $E_{red}P$ is shown partitioning between isomerization to a new 440-nm absorbing species via $k_3$ and

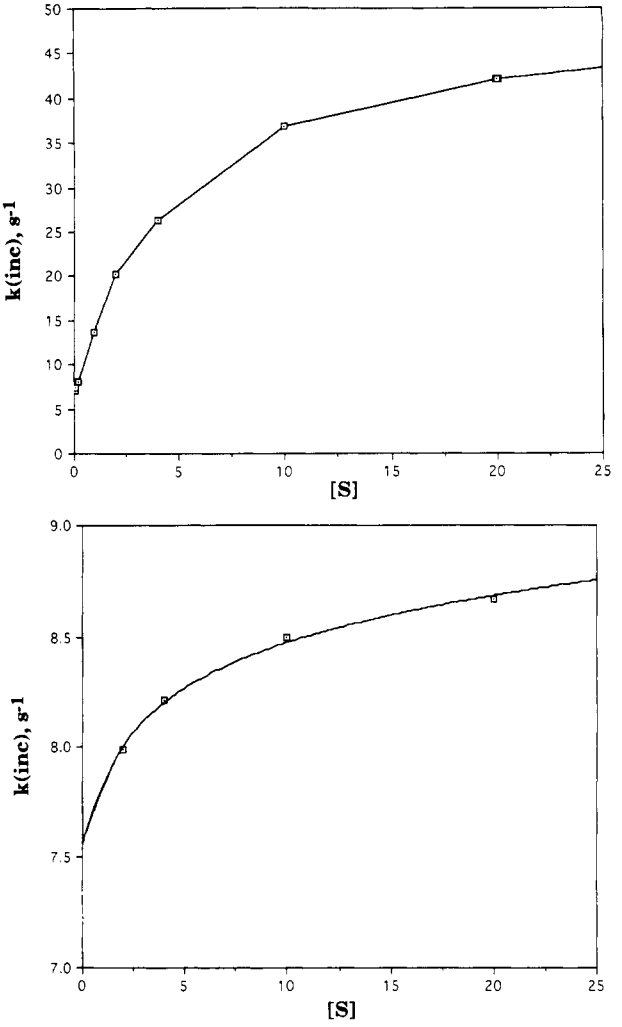


FIGURE 4: Plot of $k_{inc}$ vs [S] for *p*-hydroxybenzylamine. Shown are data for the protonated substrate (A, top) and data for [1,1-$^2H_2$]-*p*-hydroxybenzylamine (B, bottom).

$k_{-3}$ or to $E_{red}$–$NH_2$ by hydrolysis to release free aldehyde via $k_4$.

Rate expressions for the appearance and loss of $E_{red}I$ are complex and can only be derived with some limiting assumptions (cf. Bernasconi, 1976). In previous studies with BSAO using benzylamine as substrate, $k_4$ has been shown to be rapid, relative to $E_{red}P$ formation. In order to observe $E_{red}I$, $k_3$ must compete effectively with $k_4$ indicating boundary conditions of $k_3 \geq k_4 > k_2$. A second assumption is that $k_{-1} > k_2$. Although this is probably not formally correct, the magnitude of the isotope effects seen on $k_{310}$ and $k_{310}/K$ (Table II) indicates that this is an acceptable assumption. The resulting expression for the rise ($k_{inc}$) at 440 is

$$k_{inc} = \left[\frac{K_1[S]}{1 + K_1[S]}\right]k_2 + \left[\frac{k_{-2}k_{-3}}{k_{-3} + k_3}\right] \qquad (4)$$

where $K_1 = k_1/k_{-1}$.

Values for $k_{inc}$ were plotted vs [S] (Figure 4). These data were analyzed for $k_2$ and $k_{-2}k_{-3}/(k_{-3} + k_3)$, utilizing estimates for $K_1$ obtained from kinetic traces at 310 nm. Resulting values of $k_2$ for [1,1-$^1$H]- and [1,1-$^2$H]*p*-hydroxybenzylamine are summarized in Table II. As expected from the form of eq 4, rate constants for $k_{310}$ and $k_{inc}$ (440 nm) are essentially identical for [1,1-$^1$H]*p*-hydroxybenzylamine. By contrast, the estimated value for $k_{inc}$ with [1,1-$^2$H]*p*-hydroxybenzylamine is only one-third of the rate constant obtained for $k_{310}$. We

attribute this discrepancy, at least in part, to the reduced accumulation of the 440-nm species with deuterated substrate (cf. Figure 3), leading to difficulty in separating rate constants for the appearance and loss of $E_{red}I$. The failure to accumulate significant $E_{red}I$ with [1,1-$^2$H]*p*-hydroxybenzylamine suggested to us that the substrate-derived deuteron exchanged with solvent, leading to a large isotope effect on $K_2$ ($^DK_2 \simeq {}^Dk_2$) and a reduced value for $K_2 = k_2/k_{-2}$ with deuterated substrate. This idea is supported by a comparison of plots of $k_{inc}$ vs [S] for protonated (Figure 4A) vs deuterated substrate (Figure 4B), which indicate similar intercepts (5.3 and 7.6, respectively, reflecting $k_{-2}$) but different plateau values (46 and 8.9, respectively, reflecting $k_2$). It is of some interest that the average intercept value obtained for protonated and deuterated substrates from $k_{inc}$ vs [S] (Figure 4) allows an estimate of $K_2K_3$, when $K_3 > 1$; in this instance intercept = $k_{-2}/K_3$ and $k_2$/intercept = $K_2K_3$ = 6.3.

Derivation of an expression for $k_{dec}$ (440 nm) is more difficult than for $k_{inc}$ and only becomes tractable when the reaction scheme is significantly simplified. As a first approximation, we have chosen to divide the mechanism of eq 3 into kinetic and equilibrium portions:

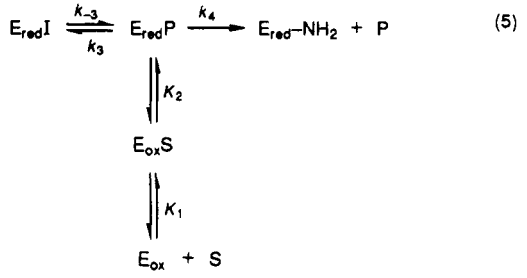


(5)

As indicated, $E_{red}P$ is assumed to be in equilibrium with $E_{ox}S$ (through $K_2$) and $E_{ox}$ + S (through $K_1$). In this way, we arrive at

$$k_{dec} = \left[\frac{K_1K_2K_3[S]}{1 + K_1[S] + K_1K_2[S] + K_1K_2K_3[S]}\right]\left[\frac{k_{-3}k_4}{k_3 + k_4}\right] \quad (6)$$

This expression predicts linear reciprocal plots of $1/k_{dec}$ vs $1/[S]$, as observed. In the likely event that $K_3 > 1$, $K_1K_2K_3$ is the largest term in the denominator and eq 6 reduces to $k_{-3}k_4/(k_3 + k_4)$ in the limit of saturating S. As originally introduced, $k_3 \geq k_4 > k_2$, such that the observed value of 6.94 $s^{-1}$ for $k_{dec}$ provides a lower limit for $k_{-3}$.[2] It appears that generation of product aldehyde is kinetically limited by the re-formation of the enzyme–product complex from an inhibitory species off the reaction path ($E_{red}I$). From the limit of low S we are able to estimate that $K_{app} = 1/K_1K_2K_3$. Since $1/K_1$ is known from the analysis of data at 310 nm, $K_2K_3$ = 8.0.[3] This can be compared to a value for $K_2K_3$ = 6.3, estimated from the analysis of $k_{inc}$.

An unexpected result is the appearance of a small (2-fold) isotope effect in $k_{dec}$, which as already discussed for $k_{inc}$ probably reflects the difficulty in extracting precise rate constants with deuterated *p*-hydroxybenzylamine. In this context it may be significant that the 3-fold increase in the isotope effect on $k_{inc}$ relative to $k_{310}$ is the same order of magnitude as the isotope effect observed on $k_{dec}$. From a mechanistic perspective, there is no reason to expect an isotope effect on the conversion of $E_{red}I$ to $E_{red}$–$NH_2$, since these steps occur subsequent to removal of the $\alpha$-hydrogen of substrate. The large inverse isotope effect on $K_{app}$ for $k_{dec}$ is quite interesting, attributed to an isotope effect on $1/K_2$ ($1/{}^DK_2 = {}^Dk_{-2}/{}^Dk_2$). The fact that this value is within a factor of 2 of $^Dk_2$ seen with numerous amines indicates that $^Dk_{-2}$ is small. A similar conclusion was reached in the analysis of $k_{inc}$, providing support for the proposal of an exchange of the substrate-derived deterium with solvent resulting from the long-lived nature of the $E_{red}P$ and $E_{red}I$ species.

Identification of $E_{red}I$ follows from (i) the chemistry of its precursor, species B, Scheme I, (ii) the fact that it is not seen with unsubstituted benzylamine or benzylamines substituted with electron-withdrawing substituents, and (iii) that a similar intermediate is observed with *p*-methoxybenyzlamine and *p*-(*N*,*N*-dimethylamino)benzylamine (see below). We propose that the product Schiff base formed from *p*- hydroxybenzylamine can undergo a tautomerization to a quinonoid intermediate:

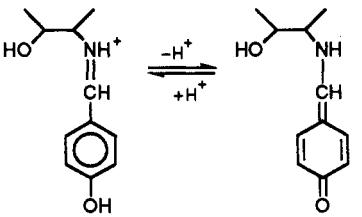


(7)

This assignment is supported by a number of literature observations, which include the characterization of $\lambda_{max}$ values for quinonoid intermediates in the reaction between substituted benzaldehydes and substituted anilines (Csaszar et al., 1978), the detection of a quinonoid intermediate (at 460 nm) during the course of substrate oxidation by tryptophan synthase (Drewe & Dunn, 19850, and the reported $\lambda_{max}$ values for quinonoid intermediates formed from dopa derivatives (Sugumaran & Semensi, 1991).

*Reaction of Bovine Serum Amine Oxidase with p-Methoxybenzylamine.* In the reaction of 5 mM *p*-methoxybenzylamine with BSAO (Figure 5), a relaxation similar to that observed for *p*-hydroxybenzylamine at 440 nm was observed. From the difference spectrum in Figure 5B, a new band, with $\lambda_{max} \approx 425$ nm, can be seen. As with the benzylamine spectrum (Figure 1), changes in optical densities at 340 and 310 nm are present. In contrast to *p*-hydroxybenzaldehyde, *p*-methoxybenzaldehyde absorbs at 285 nm, and, hence, does not interfere with the detection of the 340-nm species seen with benzylamine. Difference spectra acquired in 0.56 s (corresponding to the first approximately 10% of the reaction) indicate that the species which absorbs between 400 and 500 nm decays at approximately 51 ms from the start of data acquisition (Figure 5C). Thus, the long-wavelength intermediate formed from *p*-methyoxybenzylamine is significantly less stable than that observed with *p*-hydroxybenzylamine.

To allow for a more direct comparison of the salient features of changes in optical density at 425 nm, single-wavelength stopped-flow spectra were collected for both [1,1-$^1$H]- and [1,1-$^2$H]*p*-methoxybenzylamine (Figure 6). Much like the equivalent spectra for *p*-hydroxybenzylamine (Figure 3), Figure 6 indicates that deuterium substitution causes a decrease in the amplitude and an increase in the lifetime of the long-wavelength species. Attempts were made to analyze the data for *p*-methoxybenzylamine in a manner similar to that described for *p*-hydroxybenzylamine. However, the plot of $k_{inc}$ vs [S] for the protonated substrate displayed nonsaturation behavior while the dideuterated substrate appeared to be saturated at all substrate concentrations. These features,

[2] When $k_3 = k_4$, $k_{-3} = 2k_{obs}$.

[3] With $K_3 > 1$, $K_2 < 8$.

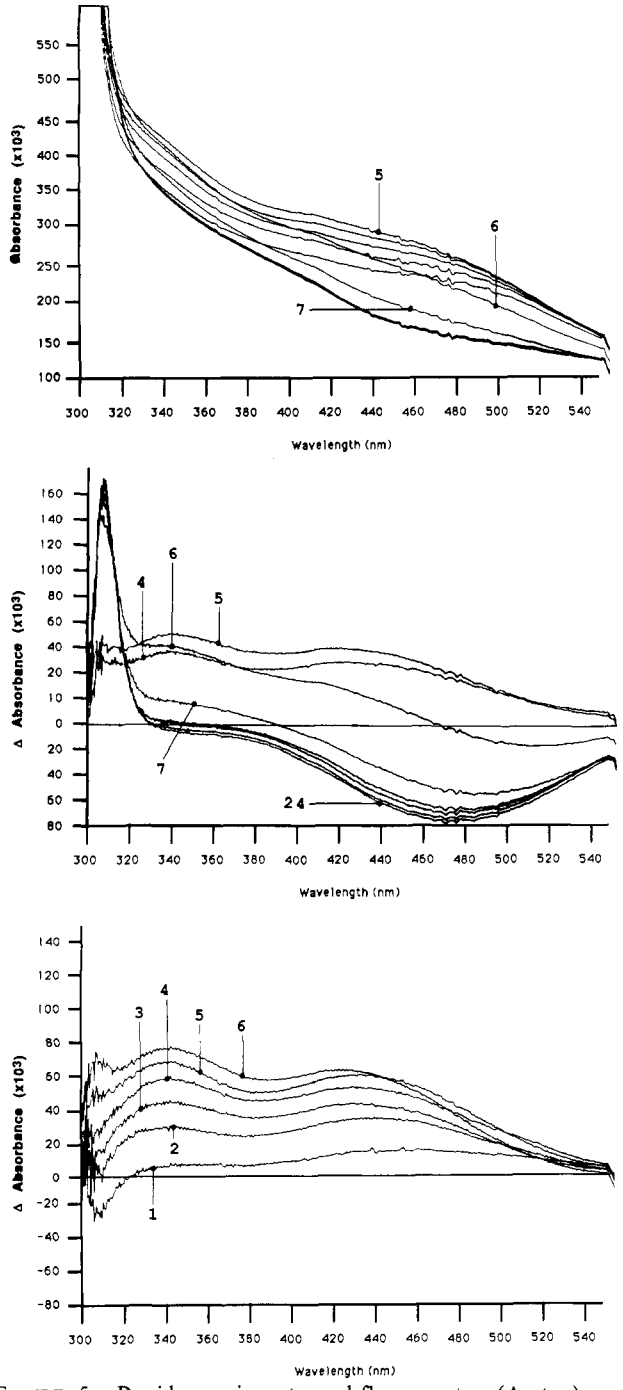


FIGURE 5: Rapid-scanning stopped-flow spectra (A, top) and difference spectra (B, middle, and C, bottom) for *p*-methoxybenzylamine showing the formation and decay of the 425-nm reaction intermediate and the formation of the species at 310 and 340 nm, attributed to reduced cofactor and Schiff base complex, respectively. These spectra were measured at 5 mM final concentration of *p*-methoxybenzylamine and 50 μM BSAO, respectively. The difference spectra in panel B illustrate scans 4, 5, 6, and 7–24 for the timing sequence described under Methods. The initiation of scanning occurred 14 ms after flow had stopped. The difference spectra in panel C illustrate a shorter data acquisition time (0.5635) and correspond to the first six scans. The initiation of scanning occurred 2 ms after flow had stopped.

together with the reduced intensity and lifetime of the 425-nm intermediate, led to kinetic parameters which were uninterpretable. We therefore restricted ourselves to a qualitative comparison of the effects of the *p*-methoxy vs *p*-hydroxy substituent. From the data in Figures 2, 3, 5, and 6, we conclude that a quinonoid species can form from *p*-methoxybenzylamine but that it absorbs at a lower wavelength and decays approximately 10 times more rapidly to $E_{red}$–$NH_2$ than the species formed from *p*-hydroxybenzylamine. These properties are as expected, given a decreased ability of the *p*-methoxy substituent to undergo stable conjugation with the imine bond of the product Schiff base complex.

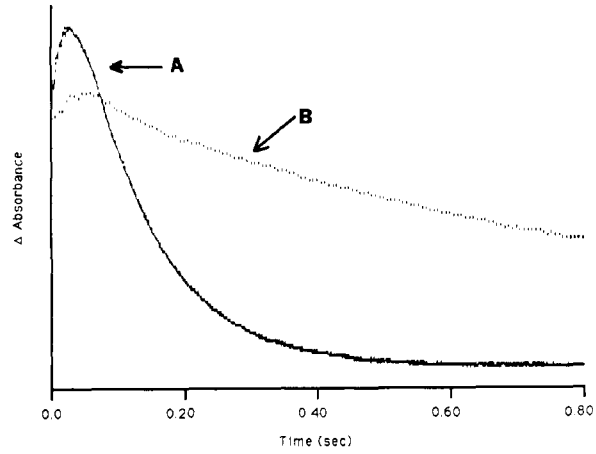


FIGURE 6: Single-wavelength absorbance traces comparing the rate of formation and decay of the spectral intermediate at 480 nm with 4 mM *p*-methoxybenzylamine (A) and 4 mM *p*-methoxy[1,1-$^2H_2$]-benzylamine (B) and 26 μM enzyme.

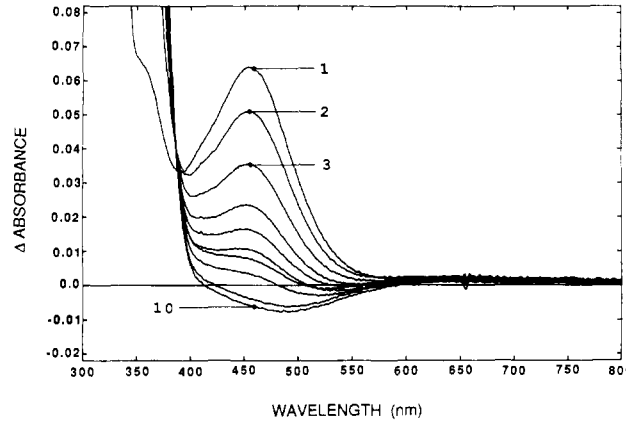


FIGURE 7: UV–visible difference spectra for *p*-(*N*,*N*-dimethylamino)-benzylamine showing the decay of the 460-nm intermediate, attributed to quinonoid intermediate. These spectra were measured at 5 mM final concentration of *p*-(*N*,*N*-dimethylamino)benzylamine and 11.7 μM BSAO, respectively. Timing of the indicated scans is as described under Methods.

*Reaction of Bovine Serum Amine Oxidase with p-(N,N-Dimethylamino)benzylamine.* It was expected that turnover of *p*-(*N*,*N*-dimethylamino)benzylamine by BSAO would generate a product–imine intermediate ($E_{red}P$) that would also be capable of quinonoid formation ($E_{red}I$). Therefore, the anaerobic, reductive half-reaction between 5 mM *p*-dimethylamino substrate and BSAO was monitored by UV–visible spectrophotometry. Although spectra could not be obtained within the 30-s hand mixing time, an intermediate was clearly observed at $\lambda_{max}$ = 460 nm, which decayed over time (Figure 7). This intermediate is similar to one previously observed in the reaction between *p*-(*N*,*N*-dimethylamino)-benzylamine and monoamine oxidase (Walker, 1987). A $t_{1/2}$ = 32.0 ± 0.9 s ($k$ = 0.020 ± 0.001 $s^{-1}$) was computed by generating a semilog plot of the decrease at 460 nm versus time, which can be compared to a turnover number of 0.026 for this substrate (Hartmann & Klinman, 1991). The difference spectra shown in Figure 7 also suggest a transiently formed species at ca. 360 nm (analogous to other substrates), which is attributed to substrate Schiff base formation. The

ability to form a quinonoid intermediate that possesses a significant half-life indicates greater stability for the intermediate derived from *p*-dimethylamino substrate than those derived from *p*-hydroxy- and *p*-methoxybenzylamines.

## CONCLUSIONS

The application of rapid-scanning stopped-flow spectroscopy to the bovine serum amine oxidase system has afforded us the opportunity to conduct an investigation of spectral changes that occur during reaction of enzyme with benzylamine, *p*-hydroxybenzylamine, *p*-methoxybenzylamine, and *p*-(*N*,*N*-dimethylamino)benzylamine. Time-resolved difference spectra, together with single-wavelength time courses, define the nature of changes in the electronic spectrum of the topa quinone (Janes et al., 1990) as the reaction of BSAO with substrates ensues (Scheme I). For the reaction of benzylamine with bovine plasma amine oxidase, rapid-scanning stopped-flow studies implicate several spectral intermediates which had not been previously observed. The species which exhibits a change in optical density at 310 nm is ascribed to reduced cofactor, on the basis of the similarity of rate constants and isotope effects for its formation to parameters previously characterized at the 480-nm band (cf. Palcic & Klinman, 1983; Hartmann & Klinman, 1991). The transiently formed spectral intermediate at 340 nm seen in the reactions of benzylamine, tyramine, and *p*-methoxybenzylamine with BSAO is concluded, on the basis of kinetic and spectral properties, to arise from Schiff base complex formation between substrate and cofactor (cf. Hartmann & Klinman, 1987). Finally, the species which dominate the *p*-hydroxybenzylamine and *p*-methoxybenzylamine rapid-scanning stopped-flow spectra and the *p*-(*N*,*N*-dimethylamino)benzylamine UV–visible spectra are ascribed to transiently formed quinonoid intermediates; this assignment is consistent with spectral changes formerly observed with pyridoxal phosphate-containing enzymes (Drewe & Dunn, 1985), complexes of amines with *para*-substituted benzaldehydes (Csaszar et al., 1978), and dopa derivatives (Sugumaran & Semensi, 1991). Although the quinonoid species lies off the reaction path, it provides evidence for its precursor, the enzyme–product Schiff base complex. As earlier studies have documented, this species is normally short lived, eluding detection.

## ACKNOWLEDGMENT

We acknowledge W. S. McIntire, at the Veteran's Administration Hospital, Department of Molecular Biology, San Francisco, CA, for assistance with single-wavelength stopped-flow experiments, M. F. Dunn, at the University of California, Department of Biochemistry, Riverside, CA, for assistance with rapid-scanning stopped-flow experiments, Dale Edmondson at Emory University, Department of Biochemistry, for samples of dimethylaminobenzylamine, and Claude Bernasconi, at the University of California, Department of Chemistry, Santa Cruz, CA, for discussions of interpretation of kinetic data.

## REFERENCES

Bernasconi, C. F. (1971) *Relaxation Kinetics*, Chaper 4, Academic Press, New York.

Császár, J., Balog, J., & Makáry, A. (1978) *Acta Phys. Chem. 24*, 373–386.

Drewe, W. F., & Dunn, M. F. (1985) *Biochemistry 24*, 3977–3987.

Farnum, M. F., Palcic, M. M., & Klinman, J. P. (1986) *Biochemistry 25*, 1898–1904.

Hartmann, C., & Klinman, J. P. (1987) *J. Biol. Chem. 262*, 962–965.

Hartmann, C., & Klinman, J. P. (1991) *Biochemistry 30*, 4605–4611.

Janes, S. M., & Klinman, J. P. (1991) *Biochemistry 30*, 4599–4604.

Janes, S. M., Mu, D., Wemmer, D., Smith, A. J., Kaur, S., Maltby, D., Burlingame, A. L., & Klinman, J. P. (1990) *Science 248*, 981–987.

Koerber, S. C., MacGibbon, A. K. H., Dietrich, H., Zepperzauer, M., & Dunn, M. F. (1983) *Biochemistry 22*, 3424–3431.

MacGibbon, A. K. H., Koerber, S. C., Pease, K., & Dunn, M. F. (1987) *Biochemistry 26*, 3058–3067.

Neumann, R., Hevey, R., & Abeles, R. H. (1975) *J. Biol. Chem. 250*, 6362–6367.

Olsson, B., Olsson, J., & Pettersson, G. (1976) *Eur. J. Biochem. 71*, 375–382.

Palcic, M. M., & Klinman, J. P. (1983) *Biochemistry 22*, 5957–5966.

Sugumaran, M., & Semensi, V. (1991) *J. Biol. Chem. 266*, 6073–6078.

Summers, M. C., Markovic, R., & Klinman, J. P. (1979) *Biochemistry 18*, 1969–1979.

Suva, R. H., & Abeles, R. H. (1978) *Biochemistry 17*, 3538–3545.

Walker, M. C. (1987) Ph.D. Thesis, Department of Biochemistry, Emory University, Atlanta, GA.

Yasunobu, K. T., Ishitaki, H., & Minamiura, N. (1976) *Mol. Cell. Biochem. 13*, 3–29.